Chapter 4

Diaza-Substituted Spirobifluorenes Having Enhanced Electron Transporting Ability for Highly Efficient Non-Doped Blue Organic Light-Emitting Diodes

4-1 Introduction

A challenge on the path to developing the high performance OLEDs is the design and synthesis of readily processible and thermally robust emissive and charge transporting materials with improved multifunctional properties.[1] OLEDs are double charge injection devices, requiring the simultaneous supply of both electrons and holes to the electroluminescent (EL) material sandwiched between two electrodes.[1a] To achieve an efficient OLED, the organic chromophore would ideally have a high luminescence quantum yield and would be efficiently facilitate the injection and transportation of electrons and holes.[2] Such demand of multifunctional capabilities from a single organic material is a formidable chancellenge to meet by currently known materials. Blue fluorophores based on distyrylarylenes,[3] anthrances,[4] spirobifluorenes,[5] oligofluorenes,[6] quinoline,[5f, 7] oxadiazole,[8] and siloles[9] have been developed for p-type (hole injection/transport) or n-type (electron injection/transport) charge semiconducting materials. Most of efficient organic fluorophores in OLEDs tend to have either hole- or electron- transport characteristics.[2]

4-2 Motivation of research

According to the material structure deign, incorporation of hole transporting triaryamine groups and electron transporting nitrogen-containing heterocyclic groups on main structure will improve the hole injection/transport ability as well as electron in OLED devices.[1] Molecules incorporate triarylamine group and nitrogen- containing heterocyclic group on π-conjugated system always exhibit high electron affinity (EA) as well as low ionization potential (IP), leading to a narrow band gap and a red shifted emission to red

region.[1c]

As showed in **Figure 4-1**, 1,10-Phenanthrolines (BPhen and BCP)[10] have been primarily used as exciton/hole-blocking layers in OLEDs owing to their deep HOMO levels (IPs ~6.5-6.7 eV) and their high electron mobilities (2.4×10^{-4} cm^2/Vs of BPhen at 1.0×10^6 V/cm, 1.1×10^{-3} cm^2/Vs of BCP at 1.0×10^6 V/cm) as well as high EAs (~3.2 eV). A 9,9'-diaryl-4,5-diazafluorenes derivative (Ansole-diazaF)[11] similar to phenanthroline was firstly used as electron-transporting and hole-blocking materials to enhance the efficiency of phosphorescent EL devices by Ono et al in 2004. In 2005, Wong *et al.* reported a more efficient OLED device with blue emission of diaza-terfluorene which incorporated 4,5-diazafluorene as the substitution group of terfluorene to facilitate electron injection from the metal cathode (**Figure 4-1**).[6d]
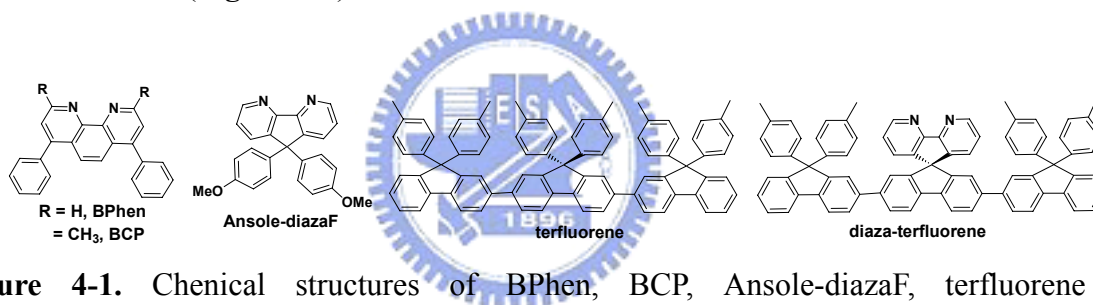

Figure 4-1. Chenical structures of BPhen, BCP, Ansole-diazaF, terfluorene and diaza-terfluorene.

In Chapter 3, we have achieved one of the best electrofluorescence blue OLEDs (ITO/NPB/**PhSPDPV**/TPBI/LiF/Al) using the efficient and bright **PhSPDPV** non-dopant material that has practically zero dipole moment and hence no problem with electric-field-induced fluorescence quenching. High device performance was due to the high PL quantum yield of **PhSPDPV**. In order to improve the electron transport and injection ability of **PhSPDPV**, which contains triarylamine group suitable only for hole transporting or injection, we introduce electron transportable and injectable diaza moiety into **PhSPDPV** (**Figure 4-2**).
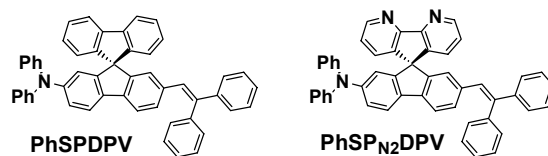
Figure 4-2. Chemical structures of **PhSPDPV** and **PhSP$_{N2}$DPV**.

4-3 Experimental

4-3-1 Materials

Synthesis of **PhSPDPV** were described in Chapter 3. Diethoxydiphenylmethyl-phosphonate[12] and 4,5-diaza-2',7'-dibromo-9,9'-spirobifluorene[6d] were synthesized according to literature procedures. 1,10-Phenanthroline monohydrate, KOH, KMnO$_4$, 2-aminobiphenyl, magnesium, bromine, diphenylamine, palladium(II) aetate (Pd(OAc)$_2$) with 47.5% palladium, tri-*tert*-butylphosphine 99% (P(^{t}Bu)$_3$), cesium carbonate (Cs$_2$CO$_3$), *n*-butyllithium (*n*-BuLi) 1.6 M in hexane, sodium hydride 60% dispersion in mineral oil (NaH), *N,N*'-dimethylformamide (DMF), tetrahydrofuran (THF), calcium hydride, benzophenone, toluene, dichloromethane, ethyl acetate, and hexane were purchased from Acros, Fluka, Aldrich, Riedel-dehaën, TCI, Merck, or Mallunckrodt. DMF was dried over calcium sulfate under reduced pressure. Toluene was distilled under nitrogen from calcium hydride. THF was distilled under nitrogen from sodium benzophenone ketyl, and the other solvents were dried using standard procedures. All other reagents were used as received from commercial sources unless otherwise stated.

4-3-2 Instrument

All of the measurement methods of instruments were similar to the description of 2-3-1 in Chapter 2.

Cyclic voltammetry experiments were performed on an Electrochemical Analysis BAS 100B with a scanning rate of 100 mV/s. Cyclic voltammetry was carried on millimolar

solutions of **PhSPDPV** and **PhSP$_{N2}$DPV** in dichloromethane with 0.1 M tetrabutylammonium perchlorate (TBAP, (^{n}Bu)$_4$NClO$_4$) electrolyte in solution.   A platinum working electrode and a 0.1 M Ag/AgNO$_3$ referenced electrode for the measurement of oxidation.   A carbon working electrode and a saturated Ag/AgCl referenced electrode for the measurement of reduction.   Ferrocene was used as an internal reference for potential calibration.

4-3-3 Synthesis

Synthersis of 4,5-diaza-2'-bromo-9,9'-spirobifluorene-7'-carboxaldehyde (BrSP$_{N2}$CHO)


BrSP$_{N2}$CHO

To a THF solution (650 mL) containing 4,5-diaza-2',7'-dibromo-9,9'-spirobifluorene (**Br$_2$SP$_{N2}$**) (4.76 g, 10.0 mmol) was added n-BuLi (4.8 mL, 12.0 mmol, 1.6M in hexane) slowly at −78 ^{o}C. The mixture was stirred for 1 h under nitrogen atmosphere. After the slow addition of DMF (2.33 mL, 30.0 mmol), the reaction solution was gradually warmed up to room temperature and kept at this temperature overnight. Saturated ammonium chloride solution was added to the reaction solution. The solution was extracted with ethyl acetate and dried over MgSO$_4$, and concentrated under reduced pressure. The residue solid was subjected to flash column chromatography (silica gel, ethyl acetate/toluene: 2/3). A white solid was obtained. Yield: 40% (1.7 g). ^{1}H NMR (400 MHz, CDCl$_3$): δ (ppm) 9.80 (s, 1H), 8.77 (dd, 2H, J = 4.6, 1.6 Hz), 7.97 (d, 1H, J = 7.8 Hz), 7.94 (dd, 1H, J = 7.9, 1.3 Hz), 7.79 (d, 1H, J = 8.2 Hz), 7.58 (dd, 1H, J = 8.2, 1.8 Hz), 7.22 (d, 1H, J = 1.3 Hz), 7.16 (d, 1H, J = 4.8 Hz), 7.14 (d, 1H, J = 4.7 Hz), 7.10 (dd, 2H, J = 7.7, 1.6 Hz), 6.89 (d, 1H, J = 1.7 Hz). ^{13}C NMR (100 MHz, CDCl$_3$): δ (ppm) 190.1, 158.8, 150.8, 149.2, 146.7, 146.5, 141.8, 139.1, 136.4, 132.1, 131.6, 130.9, 127.3, 124.8, 123.8, 123.7, 122.7, 120.8, 61.1.   TOFMS: calcd. 424.02, m/z = 425.03/427.03 (M+H$^+$).

Synthersis of 4,5-diaza-2'-diphenylamino-9,9'-spirobifluorene-7'-carboxaldehyde (PhSP$_{N2}$CHO)


PhSP$_{N2}$CHO

Under nitrogen atmosphere, a mixture of 4,5-diaza-2'-bromo-9,9'-spirobifluorene-7'-carboxaldehyde (**BrSP$_{N2}$CHO**) (1.47 g, 3.45 mmol), diphenyl- amine (0.64 g, 3.8 mmol), Pd(OAc)$_2$ (70 mg, 0.3 mmol), Cs$_2$CO$_3$ (1.24 g, 3.8 mmol), and P(^{t}Bu)$_3$ (0.12 g, 0.6 mmol) in toluene (35 mL) was heated at 120 ^{o}C with stirring 6 h. After cooling to room temperature, saturated ammonium chloride solution was added to the reaction solution. The solution was extracted with dichloromethane and dried over MgSO$_4$. The solution was concentrated under reduced pressure and subjected to flash column chromatography (silica gel, ethyl acetate/hexanes: 3/2). A yellow solid was obtained. Yield: 55% (0.98 g). ^{1}H NMR (400 MHz, CDCl$_3$): δ (ppm) 9.77 (s, 1H), 8.70 (dd, 2H, J = 4.6, 1.7 Hz), 7.89 (dd, 1H, J = 7.9, 1.4 Hz), 7.84 (d, 1H, J = 7.9 Hz), 7.10-20 (m, 9H), 7.74 (d, 1H, J = 8.4 Hz), 7.05 (dd, 1H, J = 8.4, 2.1 Hz), 6.90–7.6.98 (m, 6H), 6.42 (d, 1H, J = 2.0 Hz). ^{13}C NMR (100 MHz, CDCl$_3$): δ (ppm) 191.2, 158.9, 150.6, 149.8, 149.0, 147.9, 146.8, 142.7, 135.2, 133.7, 131.6, 129.3, 131.1, 124.7, 123.9, 123.7, 122.9, 122.2, 119.7, 117.4, 61.2. TOFMS: calcd. 513.18, m/z = 514.19 (M+H$^+$).

Synthersis of 4,5-diaza-2'-diphenylamino-7'-(2,2-diphenylvinyl)-9,9'- spirobifluorene (PhSP$_{N2}$DPV)

PhSP$_{N2}$DPV
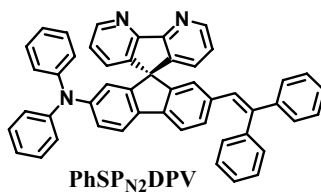
Under nitrogen atmosphere, to diethoxydiphenylmethylphosphonate (6.8 g, 22.0 mmol) in dry THF (10 mL) was added NaH (0.96 g, 60 wt% in oil, 24.0 mmol), and stirred for 1 hr at

55 ^{o}C. After cooling to room temperature, 4,5-diaza-2'-diphenylamino-9,9'-spirobifluorene-7'-carboxaldehyde (**PhSP$_{N2}$CHO**) (1.21 g, 2.36 mmol) was added, the reaction solution was heated at reflux temperature overnight. After cooling to temperature, the reaction mixture was added to water, extracted with ethyl acetate and dried over MgSO$_4$. The solution was concentrated under reduced pressure and subjected to flash column chromatography (silica gel, ethyl acetate/hexanes: 2/3). A yellow solid was obtained. Yield: 68.0% (1.06 g). ^{1}H NMR (400 MHz, CDCl$_3$): δ (ppm) 8.65 (dd, 2H, J = 4.4, 1.9 Hz), 7.57 (d, 1H, J = 8.3 Hz), 7.54 (d, 1H, J = 7.9 Hz), 7.16–7.23 (m, 5H), 7.07–7.16 (m, 9H), 6.96–7.07 (m, 4H), 6.86–6.96 (m, 8H), 6.82 (s, 1H), 6.34 (d, 1H, J = 2.0 Hz), 5.94 (s, 1H). ^{13}C NMR (100 MHz, CDCl$_3$): δ (ppm) 158.6, 150.0, 148.0, 147.7, 147.2, 145.6, 143.3, 142.6, 142.6, 140.1, 139.7, 136.5, 135.8, 131.5, 130.4, 129.6, 129.1, 128.4, 128.1, 127.5, 127.4, 127.2, 124.2, 124.1, 123.6, 123.5, 123.1, 120.8, 119.1, 118.7, 61.1. TOFMS: calcd. 663.27, m/z = 664.27 (M+H$^+$). Anal. Found (calcd.) for C$_{49}$H$_{33}$N$_3$: C 88.3 (88.66), H 5.09 (5.01), N 6.35 (6.33)
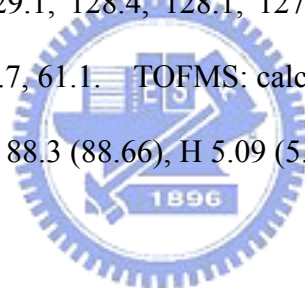
4-4 Results and Discussion

4-4-1 Synthesis

Scheme 4-1
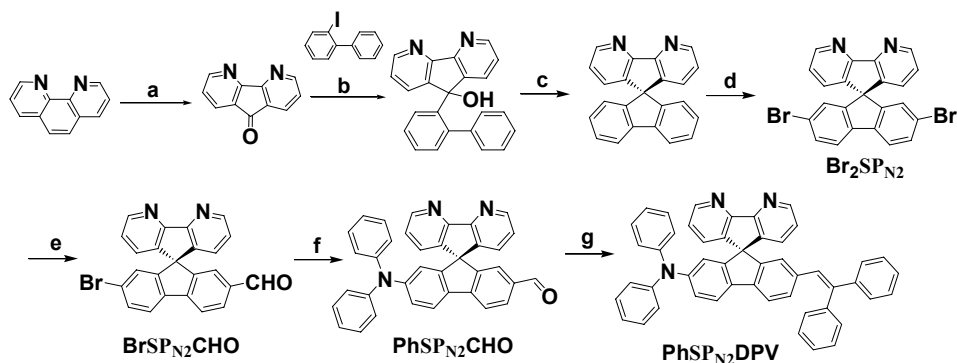
Reagents and conditions: (a) KMnO$_4$, KOH$_{(aq)}$, reflux, 40%; (b) (i) Mg, THF, (ii) 4,5-diazafluore-9-one, THF, reflux, 84%; (c) H$_2$SO$_4$, HOAc, reflux, 94%; (d) Br$_2$, FeCl$_3$, CH$_2$Cl$_2$, rt, 84%; (e) (i) nBuLi, THF, −78 ^{o}C; (ii) DMF, rt, 40%; (f) Ph$_2$NH, Cs$_2$CO$_3$, Pd(OAc)$_2$, P(tBu)$_3$, toluene, 120 ^{o}C, 55%; (g) NaH, diethoxydiphenylmethyl- phosphonate, THF, reflux, 68%.

As showed in Scheme 1, the synthetic strategy of **PhSP$_{N2}$DPV** was similar to **PhSPDPV** as described in Chapter 3. The known compound **Br$_2$SP$_{N2}$** was synthesized from the commercial available starting material 1,10-phenanthrene in four steps following the literature procedure[6d]. The total isolated yield of **Br$_2$SP$_{N2}$** was 26%. The isolated yields of **BrSP$_{N2}$CHO**, **PhSP$_{N2}$CHO** and **PhSP$_{N2}$DPV** always lower than those without diaza-substituted compounds. Particularly, problem associated with the formylation of **Br$_2$SP$_{N2}$** was observed. The low yield of **BrSP$_{N2}$CHO** may be due to the difficulty in the dissolving of **Br$_2$diazaSP** in THF under −78 ^{o}C. In addition to the low solubility, the pronounced tailing bands of diaza series compounds in column chromatography lead to the relative low isolated yields.

4-4-2 Thermal properties

Table 4-1. Thermal properties of PhSPDPV and PhdiazaSPDPV

	$T_m\,(^{o}C)$	$T_g\,(^{o}C)$	$T_c\,(^{o}C)$	$T_d\,(^{o}C)$
PhSPDPV	223	112	Not observed	405
PhSP$_{N2}$DPV	249	113	Not observed	413

[a]Melt transition temperature only observed in the first heating scan.

The data of thermal analysis by DSC and TGA of **PhSPDPV** and **PhSP$_{N2}$DPV** are summarized in **Table 4-1**. The repeat heating/cooling DSC scans of **PhSPDPV** and **PhSP$_{N2}$DPV** were shown in **Figure 4-3**. **PhSP$_{N2}$DPV** shows a glass transition (T_g) at 113 ^{o}C, which is very close to 112 ^{o}C of **PhSPDPV**. Melting transition temperature (T_m) were observed for both blue spirobifluorene derivatives but only in the first heating scan of DSC, **PhSP$_{N2}$DPV** showed T_m 16 ^{o}C higher than that of **PhSPDPV**. A higher onset of the decompose temperature (T_d) was observed for **PhSPDPV** than **PhSP$_{N2}$DPV**. The high T_g and T_d values make these two blue emitter suitable for the application of OLEDs.
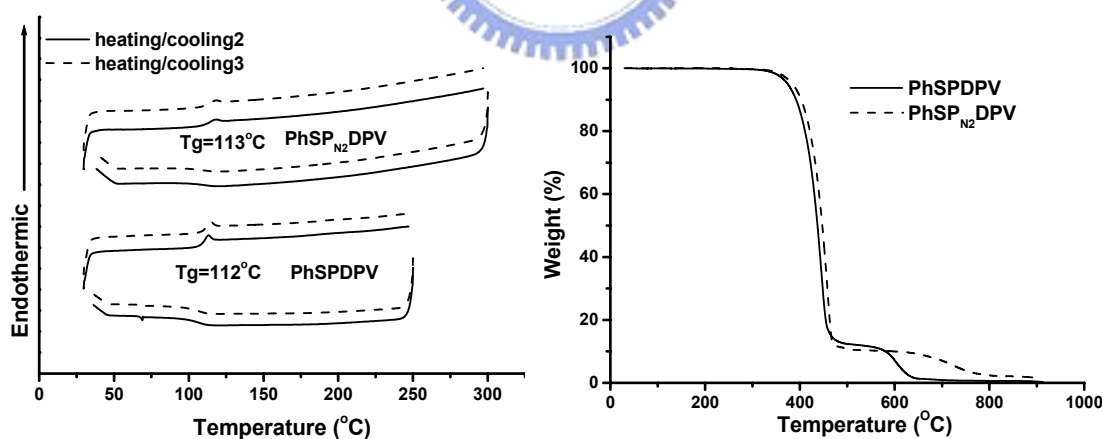

Figure 4-3. DSC and TGA scans of **PhSPDPV** and **PhSP$_{N2}$DPV**.

4-4-3 Photophysical properties and energy levels

Table 4-2 summarizes the optical characteristics of two blue spirobifluorene derivatives. **Figure 4-4** shows the UV-vis absorption and photoluminescence (PL) spectra in chlorobenzene and as the thin film of **PhSPDPV** and **PhSP$_{N2}$DPV**, respectively. Both of

PhSPDPV and **PhSP$_{N2}$DPV** exhibit very similar spectroscopic: nearly the same lowest-energy absorption bands (around 385-386 nm in chlorobenzene, 390-388 nm in thin film); similar PL spectra either in chlorobenzene (468-470 nm) or as thin film (468-478 nm). Compared with **PhSPDPV**, which the slight red-shifting of the emission spectra of **PhSP$_{N2}$DPV** maybe attributed to the small intramolecular charge transfer (ICT) between the diphenylamino donor and diazafluorene units of **PhSP$_{N2}$DPV**. **PhSPDPV** and **PhSP$_{N2}$DPV** emit relatively bright blue fluorescence in solution (Φ_f = 60-66%) or in solid state (Φ_f = 51-43%).

Table 4-2. Optical properties as well as energy levels of **PhSPDPV** and PhSP$_{N2}$DPV.

	Solution			Solid state			ΔE (eV, nm) [b]	HOMO/ LUMO (eV/eV) [c]
	λ_{max}^{ab} (nm)[a]	λ_{max}^{fl} (nm)[a]	Φ_f %[a]	λ_{max}^{ab} (nm)	λ_{max}^{fl} (nm)	Φ_f (%)		
PhSPDPV	385	468	60	390	467	51	2.80, 442	5.50/2.70
PhSP$_{N2}$DPV	386	470	66	388	478	43	2.78, 446	5.51/2.73

[a]In chlorobenzene. [b]ΔE is the band-gap energy estimated from the low energy edge of the thin film absorption spectra. [c]HOMOs was measured from AC-2, LUMO = HOMO − ΔE.
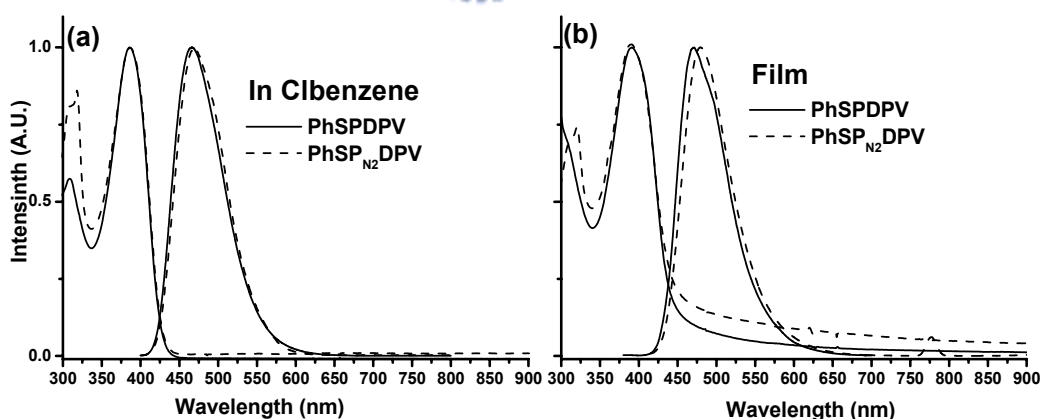

Figure 4-4. Normalized UV-vis absorption and photoluminescence spectra of **PhSPDPV** and **PhSP$_{N2}$DPV**; (a) In chlorobenzene solution and (b) solid film.

The potential energy of HOMO and LUMO of **PhSPDPV** and **PhSP$_{N2}$DPV** is summarized in **Table 4-2**. It can be found that the HOMO energy level of both fluorophore

is mainly determined by the arylamino substituted and little to do with diaza moiety.   Almost the same HOMO energy levels of blue spirobifluorene derivatives (only 0.01 eV different) were determined by low energy photo-electron spectrometer (AC-2).   The optical energy gaps estimated from the low energy edge of film absorption spectra, a slightly smaller band gap was observed by **PhSP$_{N2}$DPV**.   Due to the diaza moiety, **PhSP$_{N2}$DPV** was expected to have better electron injection ability than **PhSPDPV** due to the lower LUMO level of **PhSP$_{N2}$DPV**.   The same blue OLED with configuration of ITO/NPB (10 nm)/**PhSP$_{N2}$DPV** (40 nm)/TPBI (50 nm)/LiF (1 nm)/Al (150 nm) was adopted in order to compare to the performance of **PhSPDPV** in Chapter 3.
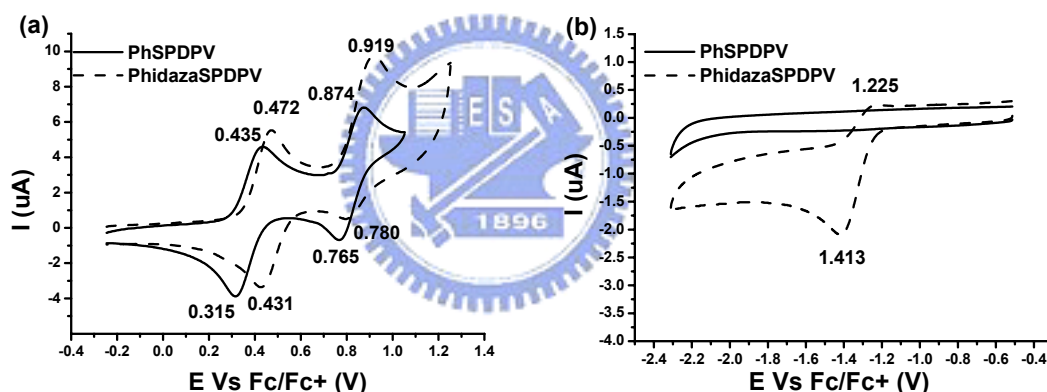
4-4-4 Electrochemistry

Figure 4-5. (a) Oxidation and (b) reduction of cyclic voltammograms of **PhSPDPV** and **PhSP$_{N2}$DPV** in dichloromethane/0.1 M (^{n}Bu)$_4$NClO$_4$ solution.

Figure **4-5** show the oxidation and reduction potential of **PhSPDPV** and **PhSP$_{N2}$DPV**.   **PhSPDPV** has a lower oxidative potential level than **PhSP$_{N2}$DPV**, and there is no reduction signal was detectable for **PhSPDPV**.   It is reasonable that **PhSPDPV** would show a higher HOMO level than **PhSP$_{N2}$DPV**, of which hole would be injected easier from anode to **PhSPDPV** than **PhSP$_{N2}$DPV** in OLEDs.

4-4-5 OLEDs Characterization

4-4-5-1 High performance blue devices

Table 4-3. Characteristics of non-dopant OLEDs of **PhSPDPV** and **PhSP$_{N2}$DPV**.

	Max. Luminance (cd/m^2)	Luminance, Efficiency, Voltage (cd/m^2,%, V)[b]	Max. Efficiency (%, cd/A, lm/W)	λ_{max}^{el} (nm)	CIE 1931 Chromaticity (x, y)
PhSPDPV[a]	33018	910, 2.9, 4.7	3.4, 5.4, 5.7	478	0.14, 0.22
PhSP$_{N2}$DPV[a]	60506	1811, 4.4, 5.17	4.9,10.2, 10.5	480	0.16, 0.32

[a]Devices have the configuration of ITO/NPB (10 nm)/**emitter** (40 nm)/TPBI (50 nm)/LiF (1 nm)/Al (150 nm) referring to those in **Figure 4-6(a)**.   [b]At current density of 20 mA/cm^2

Non-dopant blue OLED ITO/NPB (10 nm)/**PhSP$_{N2}$DPV** (40 nm)/TPBI (50 nm)/LiF (1 nm)/Al (150 nm) was fabricated by thermal vacuum deposition similar to the fabrication of **PhSPDPV**.   The data of devices was summarized in **Table 4-3** including the device data of **PhSPDPV** from Chapter 3. High performance blue EL was observed for both devices (**Figure 4-6**) and the wavelength of EL is very close to that of solid-state PL.   Device with **PhSP$_{N2}$DPV** displays the higher electroluminance (L) of 60500 cd/m^2 and the higher maximum external quantum efficiency (η_{EXT}) of 4.9% than that of **PhSPDPV** device (Figure 4-6(b)).   By checking the solid state fluorescence quantum yield of these two blue fluorophores, fluorescence quantum yield of **PhSP$_{N2}$DPV** (Φ_f = 43%) was lower than that of **PhSPDPV** (Φ_f = 50%).   One intriguing question is why the low fluorescence quantum yield **PhSP$_{N2}$DPV** outperforms high fluorescence quantum yield **PhSPDPV** in OLEDs?   It might be attributed to the enhancement of electron transporting and electron injecting ability due to the 4,5-diazafluorene moiety that enhances the charge recombination in OLED with balanced carrier transporting ability. Following is the supporting evidence of our theory.
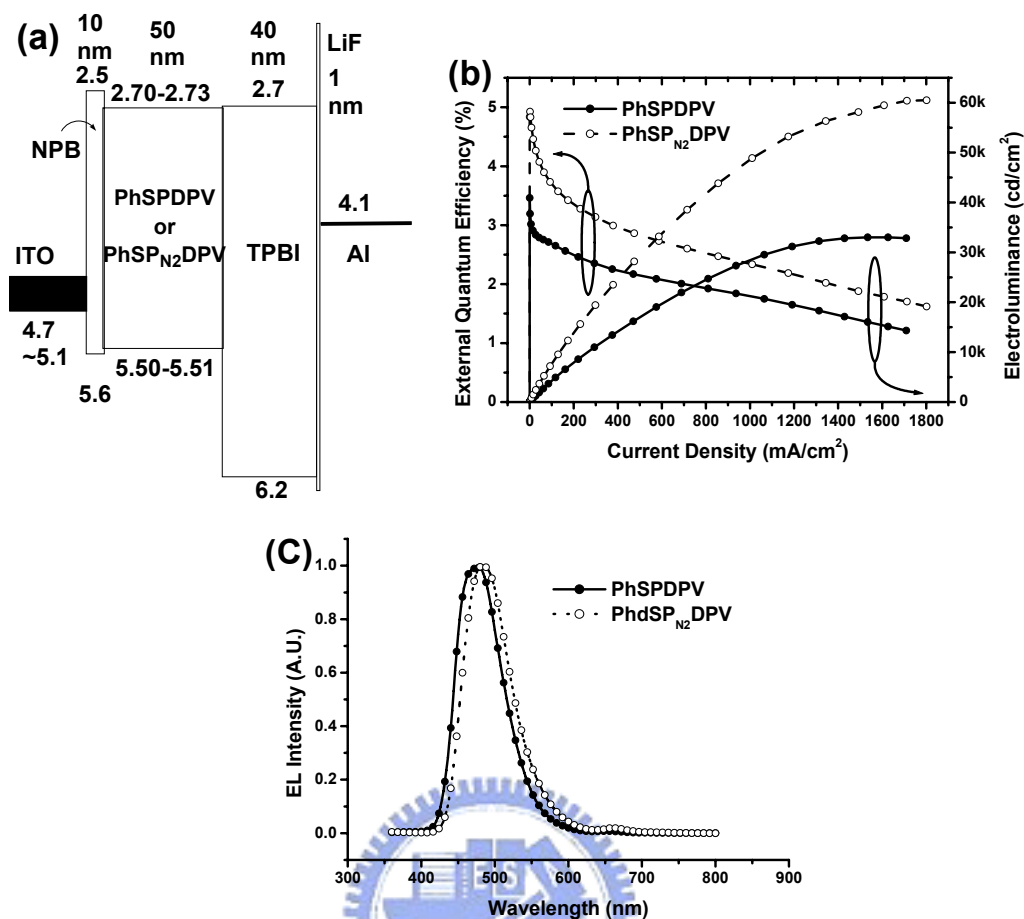
Figure 4-6. Electroluminescence (EL) characteristics of blue non-dopant OLEDs based on **PhSPDPV** and **PhSP$_{N2}$DPV**: (a) Relative energy-level alignments and layer thickness of OLEDs; (b) Efficiency-current density-electroluminescence (η_{EXT}-*I-L*) characteristics of devices; (c) The EL spectra of devices.

4-4-5-2 Current Density-Voltage characteristic of electron or hole only devices

Together with other materials adopted in the electron or hole only devices fabrication, relative energy-level alignments and layer thickness of devices are schematically depicted in **Figure 4-6**. Electron-only devices were fabricated and characterized with the configuration of ITO/BCP/**PhSPDPV** or **PhSP$_{N2}$DPV**/TPBI/ LiF/Al. TPBI and BCP layers were employed as electron transporting layer and hole-blocking layer, respectively, resulting only electron carriers go through the device from cathode to anode. Figure 4-7 shows *I-V* characteristics of the electron-only devices. It reveals that the electron-only device of **PhSP$_{N2}$DPV** has a lower current turn-on voltage and higher current density under the same

118

applied voltage than **PhSPDPV**. The poor *I-V* quality of **PhSPDPV** might be attributed to the lower electro-transporting ability of **PhSPDPV**.
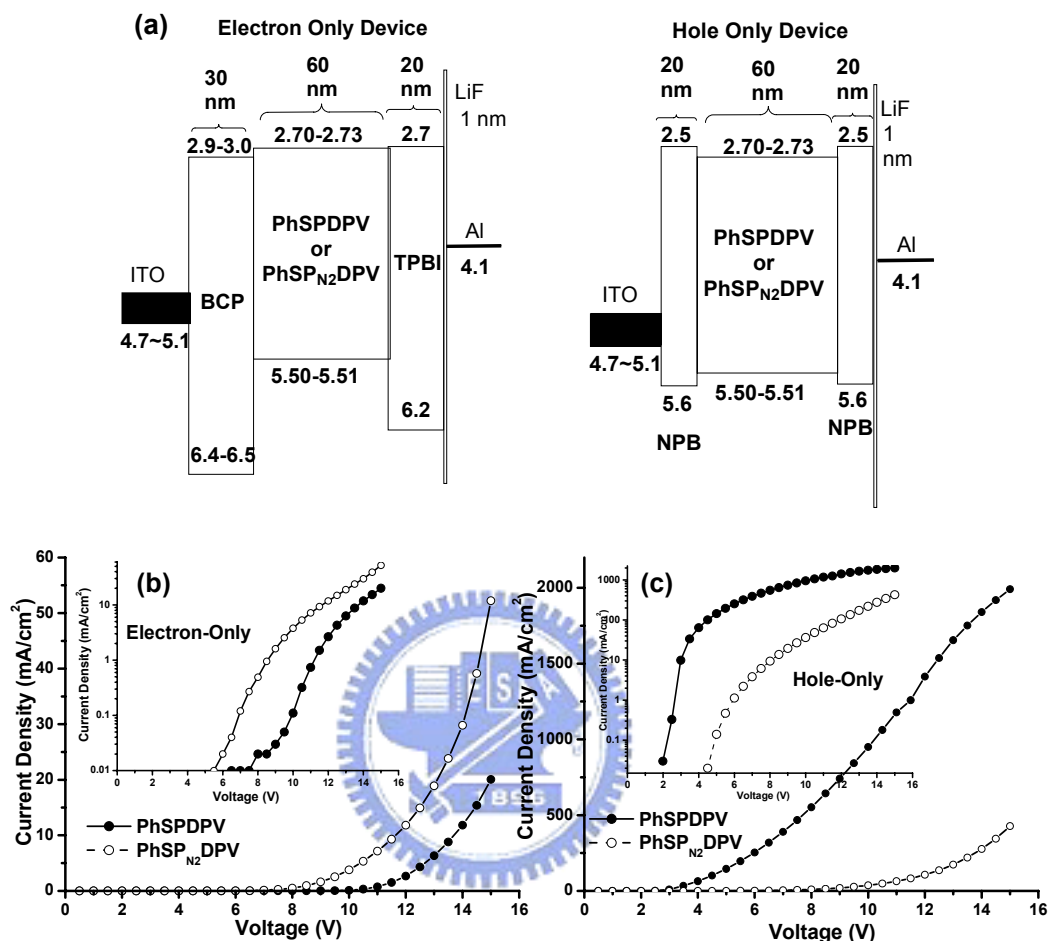

Figure 4-7. (a) Relative energy-level alignments and layer thickness of carrier only devices; Current density-voltage (*I-V*) characteristics of carrier-only devices: (b) electron-only device, and (c) hole-only device.

This result can be rationalized by the smallest energy barrier between the LUMO's of **PhSP$_{N2}$DPV** and TPBI, which provides an effective pathway for electron injection from TPBI to **PhSP$_{N2}$DPV** and the easily electron transportable diaza moiety of **PhSP$_{N2}$DPV**. Hole-only devices were fabricated and characterized with a configuration of ITO/NPB/**PhSPDPV** or **PhSP$_{N2}$DPV**/NPB/LiF/Al. NPB layer close to cathode was employed as a electron-blocking layer that only hole carriers go through the device from anode to cathode. These *I-V* characteristics of the hole-only devices are shown in **Figure**

4-7.   It is evident that **PhSP$_{N2}$DPV** device has lower current density under the same applied voltage than does **PhSPDPV**.   Both spirobifluorene derivatives shown similar HOMO energy level lead to the same hole injected from NPB layer (close to anode) into spirobifluorene derivative layer.   The poor *I-V* quality of **PhSP$_{N2}$DPV** might be attributed to the lower hole-transporting ability of **PhSP$_{N2}$DPV**.

4-4-5-3 PhSPDPV and PhSP$_{N2}$DPV OLED test

Table 4-4. Characteristics of non-dopant OLEDs of **PhSPDPV** and **PhSP$_{N2}$DPV**.

Emitter	Max. Luminance (cd/m^2)	Luminance, Efficiency, Voltage (cd/m^2,%, V)[d]	Max. Efficiency (%, cd/A, lm/W)	λ_{max}^{el} (nm)	CIE 1931 Chromaticity (x, y)
PhSPDPV[a]	132	1, 0.003, 4.1	0.009, e, e	464	0.14, 0.17
PhSPDPV[b]	9697	584, 2.3, 4.5	2.7, 3.5, 3.6	460	0.14, 0.16
PhSPDPV[c]	152	0, 0, 2.7	0.004, e, e	472	0.15, 0.22
PhSP$_{N2}$DPV[a]	32447	951, 2.8, 3.9	2.9, 5.0, 5.2	474	0.15, 0.25
PhSP$_{N2}$DPV[b]	13502	515, 1.3, 6.4	1.4, 3.0, 2.1	482	0.15, 0.32
PhSP$_{N2}$DPV[c]	8996	306, 0.77, 6.8	0.78, 1.55, 1.4	484	0.15, 0.31

[a]ITO/NPB (40 nm)/**PhSPDPV** or **PhSP$_{N2}$DPV** (40 nm)/LiF (1 nm)/Al (150 nm); [b]ITO/**PhSPDPV** or **PhSP$_{N2}$DPV** (40 nm)/TPBI (40 nm)/LiF (1 nm)/Al (150 nm); [c]ITO/**PhSPDPV** or **PhSP$_{N2}$DPV** (80 nm)/LiF (1 nm)/Al (150 nm); [d]At current density of 20 mA/cm^2; [e]The value is smaller than 0.01.
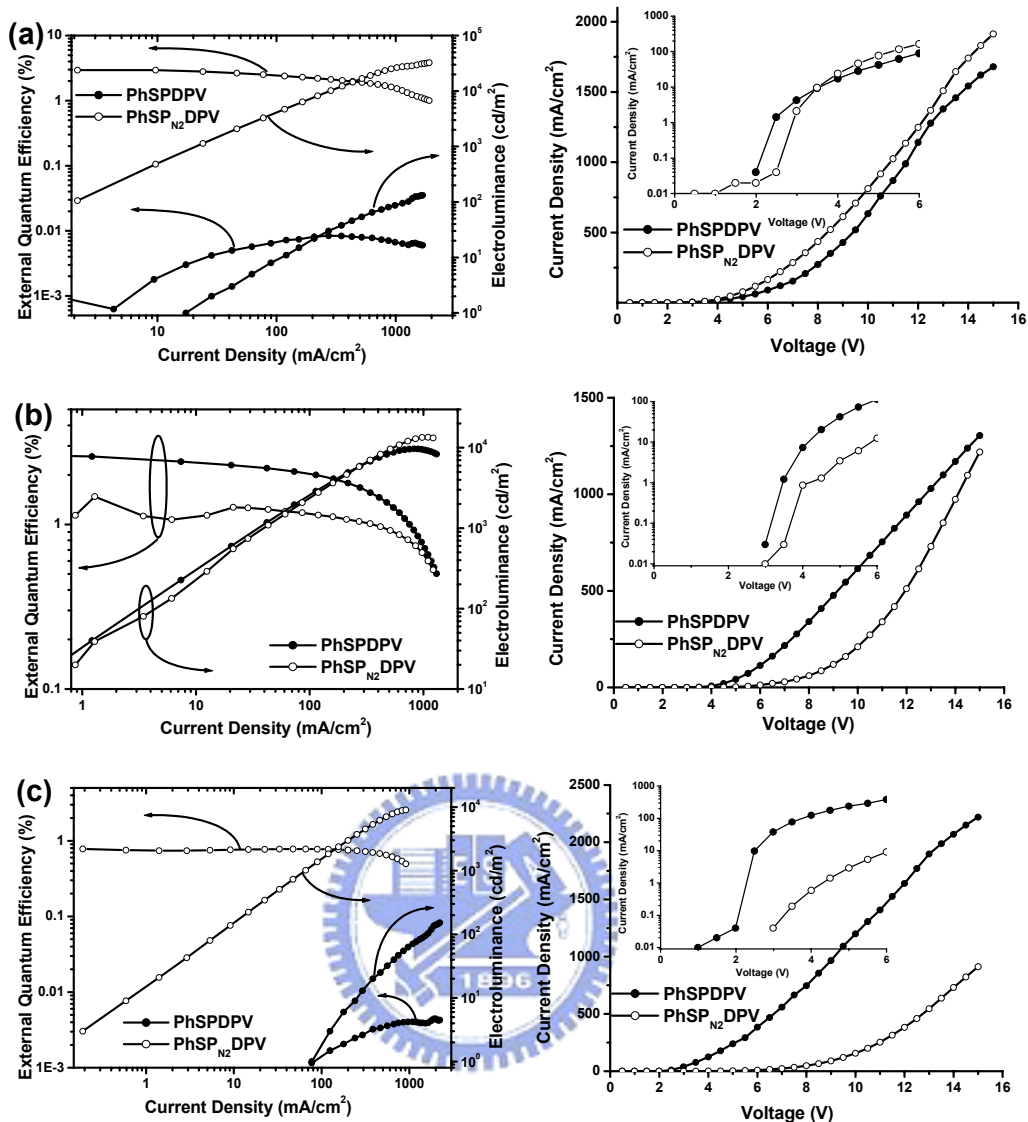
Figure 4-8. Efficiency-current density-electroluminescence (η_{EXT}-I-L) and Current density-voltage (I-V) characteristics of devices. (a) ITO/NPB (40 nm)/**PhSPDPV** or **PhSP$_{N2}$DPV** (40 nm)/LiF (1 nm)/Al (150 nm); (b) ITO/**PhSPDPV** or **PhSP$_{N2}$DPV** (40 nm)/TPBI (40 nm)/LiF (1 nm)/Al (150 nm); (c) ITO/**PhSPDPV** or **PhSP$_{N2}$DPV** (80 nm)/LiF (1 nm)/Al (150 nm)

Having high fluorescence quantum yields but different charge-transporting properties **PhSPDPV** and **PhSP$_{N2}$DPV**, were subjected to EL studies using different device structures on an ITO anode. NPB and TPBI were used as hole transporting and electron transporting materials, respectively, while LiF and Al were used the electron injecting layer and the cathode. Three series device structures were fabricated. The first type is ITO/NPB (40 nm)/**PhSPDPV** or **PhSP$_{N2}$DPV** (40 nm)/ LiF (1 nm)/Al (150 nm), where **PhSPDPV** or

PhSP$_{N2}$DPV was adopted as both electron-transporting and light-emitting material. The second type is ITO/**PhSPDPV** or **PhSP$_{N2}$DPV** (40 nm)/TPBI (40 nm)/LiF (1 nm)/Al (150 nm), while **PhSPDPV** or **PhSP$_{N2}$DPV** was adopted as a hole-transporting and light-emitting material. The third thpe is a single layer device ITO/**PhSPDPV** or **PhSP$_{N2}$DPV** (80 nm)/LiF (1 nm)/Al (150 nm), where **PhSPDPV** or **PhSP$_{N2}$DPV** was adopted as light-emitting material as well as either electron-transporting or hole-transporting material. The device performances are summarized in **Table 4-4**.

Efficiency-current density-electroluminance (η_{EXT}-I-L) characteristics of three types of OLEDs are shown in **Figure 4-8**. As shown in **Figure 4-8(a)** and **(c)**, **PhSP$_{N2}$DPV** OLEDs exhibited significantly better performance than did **PhSPDPV** OLEDs, when **PhSP$_{N2}$DPV** was adopted as both electron-transporting and light-emitting layer or simply bipolar light-emitting layer. In **Figure 4-8(b)**, the device performance of **PhSP$_{N2}$DPV** was slightly inferior to that of **PhSPDPV**. This is consistent with our experimental observation that **PhSP$_{N2}$DPV** is an efficient light-emitting material with electron-transporting.

In the first type of the device, **PhSPDPV** OLED has a higher current density than **PhSP$_{N2}$DPV** at applied voltage less than 3.5 V. Such result can be rationalized by the easier hole injection from hole transporting NPB to **PhSPDPV** than **PhSP$_{N2}$DPV**. The cyclic voltammetry (CV) measurement provided a good evidence that **PhSPDPV** has a lower ionization potential (IP) value (0.38 V vs Fc/Fc$^+$) than **PhSP$_{N2}$DPV** (0.45 V vs Fc/Fc$^+$). However, **PhSP$_{N2}$DPV** OLED had a higher current density than **PhSPDPV** at applied voltage more than 3.5 V. This might be due to the diaza electro-transporting moiety of **PhSP$_{N2}$DPV** that lowers the LUMO energy level closer to the work function of cathode. At elevated applied voltage, **PhSP$_{N2}$DPV** OLED has relatively more electron injection than **PhSPDPV** OLED. High performance blue **PhSP$_{N2}$DPV** OLED displays a higher electroluminance of 32447 cd/m^2 and higher maximum external quantum efficiency of 2.9% than those of **PhSPDPV** OLED. **PhSP$_{N2}$DPV** OLED significantly outperforms **PhSPDPV** (300 fold

better).　The superior OLED performance of **PhSP$_{N2}$DPV** over **PhSPDPV** is a clear evidence that diaza moiety plays an important role of improving of electron-transporting and electron-injection.

　　In the second type of OLEDs, the hole carrier was limited in front of TPBI hole-blocking and electron-transporting layer.　This greatly improved the performance (efficiency and current density) of **PhSPDPV** OLED.　Similar to the first type of devices, the current density of **PhSP$_{N2}$DPV** OLED started a sharp increase when the applied voltage is higher than 12 V. This can be contributed to the enhancement of electron transporting ability of **PhSP$_{N2}$DPV** due to the diaza moiety.　Among three types of the devices, **PhSPDPV** outperformed **PhSP$_{N2}$DPV** only in the second type of OLEDs.　This is because that the configuration of the second type will favor hole-transporting **PhSPDPV** more than electron-transporting **PhSP$_{N2}$DPV**.

　　For the third type of the devices (single-layer devices without hole-blocking or electron-blocking layer), both **PhSPDPV** and **PhSP$_{N2}$DPV** exhibited very poor OLED performance because of the waste of hole or electron carrier on the contact electrodes. Nevertheless, for these two poor single-layer devices, **PhSP$_{N2}$DPV** OLED once again outperformaned **PhSPDPV** OLED in terms of maximum external quantum efficiency (0.78% vs 0.004%).　Similarly, diaza moiety is the key factor, which provides material an enhanced electron-transporting ability and an improved charge balanced in OLED.

4-5 Conclusions

　　In summary, we have successfully designed and synthesized **PhSPDPV** and **PhSP$_{N2}$DPV** for efficient non-doped blue OLEDs.　The thermal, optical physical, electrochemical and electroluminescent properties were investigated.　The electron transporting and electron injecting ability of both materials were also investigated.　We have proven that **PhSP$_{N2}$DPV** has enhanced properties due to diaza moiety as part of the

spirobifluorene structure.　It can improve the electron transportation that facilitates hole-electron charge recombination leading to more charge balance in **PhSP$_{N2}$DPV** OLED. Compared with **PhSPDPV** OLED, a significantly improved OLED performance was achieved for **PhSP$_{N2}$DPV** (maximum brightness of 60500 cd/m^2 and maximum η_{EXT} of 4.9%).

4-6 References

[1]　(a) Hung, L. S.; Chen, C. H. *Mater. Sci. Eng.* **2002**, *R39*, 143.; (b) Hughes, G.; Bryce, M. R. *J mater. Chem.* **2005**, *15*, 94.; (c) Kulkarni, A. P.; Tonzola, C. J.; Babel, A.; Jenekne, S. A. *Chem. Mater.* **2004**, *16*, 4556.; (d) Segura, J. L. *Acta. Polym.* **1998**, *49*, 319.; (e) Hsieh, B. R. *Macromol. Symp.* **1997**, *125*, 49.; (f) Chen, C.-H. *Chem. Mater.* **2004**, 16, 4389.; (g) Mischke, U.; Bäuerle, P. *J. Mater. Chem.* **2000**, *10*, 1471.

[2]　(a) Tang, C. W.; VanSlyke, S. A. *Appl. Phys. Lett.* **1987**, *51*, 913.; (b) Burroughes, J. H.; Bradley, D. D. C.; Brown, A. R.; Marks, R. N.; Mackay, K.; Friend, R. H.; Burns, P. L.; (c) Holmes, A. B. *Nature* **1990**, *347*, 539. Braun, D.; Heeger, A. J. *Appl. Phys. Lett.* **1991**, *58*, 1982.; (d) Kraft, A.; Grimsdale, A. C.; Holmes, A. B. *Angew. Chem., Int. Ed.* **1998**, *37*, 402.; (e) Bernius, M. T.; Inbasekaran, M.; O'Brien, J.; Wu, W. *Adv. Mater.* **2000**, *12*, 1737.; (f) Kim, D. Y.; Cho, H. N.; Kim, C. Y. *Prog. Polym. Sci.* **2000**, *25*, 1089.; (g) Rees, I. D.; Robinson, K. L.; Holmes, A. B.; Towns, C. R.; O'Dell, R. *MRS Bull.* **2002**, *27*, 451.; (h) Friend, R. H.; Gymer, R. W.; Holmes, A. B.; Burroughes, J. H.; Marks, R. N.; Taliani, C.; Bradley, D. D. C.; Dos Santos, D. A.; Brédas, J. L.; Lögdlund, M.; Salaneck, W. R. *Nature* **1999**, *397*, 121.

[3]　(a) Hosokawa, C.; Higashi, H.; Nakamura, H.; Kusumoto, T. *Appl. Phys. Lett.* **1995**, *67*, 3853.; (b) Shaheen, S. E.; Jabbour, G. E.; Morell, M. M.; Kawabe, Y.; Kippelen, B.; Peyghambarian, N.; Nabor, M.-F.; Schlaf, R.; Mash, E. A.; Armstrong, N. R. *J. Appl. Phys.* **1998**, *84*, 2324.; (c) Lee , M.-T.; Chen, H.-H.; Liao, C.-H.; Tsai, C.-H.; Chen, C. H.

Appl. Phys. Lett. 2004, **85**, 3301.; (d) Kishigami, Y.; Tsubaki, K.; Kondo, Y.; Kido, J. *Synth. Met.* **2005**, *153*, 241.

[4]   (a) Shi, J.; Tang, C. W. *Appl. Phys. Lett.* **2002**, *80*, 3201.; (b) Gebeyehu, D.; Walzer, K.; He, G.; Pfeiffer, M.; Leo, K.; Brandt, J.; Gerhard, A.; Stößel,P.; Vestweber, H. *Synth. Met.* **2005**, *148*, 205.; (c) Li, Y.; Fung, M. K.; Xie, Z.; Lee, S.-T.; Hung, L.-S.; Shi, J. *Adv. Mater.* **2002**, *14*, 1317.; (d) Kan, Y.; Wang, L.; Duan, L.; Hu, Y.; Wu, G.; Qiu, Y. *Appl. Phys. Lett.* **2004**, *84*, 1513.; (e) Kim, Y.-H.; Jeong, H.-C.; Kim, S.-H.; Yang, K.; Kwon, S.-K. *Adv. Funct. Mater.* **2005**, *15*, 1799.

[5]   (a) Salbeck, J.; Yu, N.; Bauer, J.; Weissortel, F.; Bestgen, H. *Synth. Met.* **1997**, *91*, 209.; (b) Kim, Y.-H.; Shin, D.-C.; Kim, S.-H.; Ko, C.-H.; Yu, H.-S.; Chae, Y.-S.; Kwon, S.-K. *Adv. Mater.* **2001**, *13*, 1690. (c) Tao, S.; Peng, Z.; Zhang, X.; Wang, P.; Lee, C.-S.; Lee, S.-T. *Adv. Funct. Mater.* **2005**, *15*, 1716. (d) Shen, W.-J.; Dodda, R.; Wu, C.-C.; Wu, F.-I.; Liu, T.-H.; Chen, H.-H.; Chen, C. H.; Shu, C.-F. *Chem. Mater.* **2004**, *16*, 930.; (e) Wu, C. C.; Lin, Y. T.; Chiang, H. H.; Cho, T.-Y.; Chen, C.-W.; Wong, K.-T.; Liao, Y.-L.; Lee, G.-H.; Peng, S.-M. *Appl. Phys. Lett.* **2002**, *81*, 577.; (f) Chen, C.-H.; Wu, F.-I.; Shu, C.-F.; Chien, C.-H.; Tao, Y.-T. *J. Mater. Chem.* **2004**, *14*, 1585.

[6]   (a) Wu, C.-C.; Lin, Y.-T.; Wong, K.-T.; Chen, R.-T.; Chien, Y.-Y. *Adv. Mater.* **2004**, *16*, 61.; (b) Li, T.; Yamamoto, T.; Lan, H.-L.; Kido, J. *Polym. Adv. Technol.* **2004**, *15*, 266.; (c) Markham, J. P. J.; Namdas, E. B.; Anthopoulos, T. D.; Samuel, I. D. W.; Richards, G. J.; Burn, P. L. *Appl. Phys. Lett.* **2004**, *85*, 1463.; (d) Wong, K.-T.; Chen, R.-T.; Fang, F.-C.; Wu, C.-C.; Lin, Y.-T. *Org. Lett.* **2005**, *7*, 1979.

[7]   Tonzola, C. J.; Kulkarni, A. P.; Gifford, A. P.; Kaminsky, W.; Jenekhe, S. A. *Adv. Mater.* **2007**, *17*, 864.

[8]   Chan, L.-H.; Lee, R.-H.; Hsieh, C.-F.; Yeh, H.-C.; Chen, C.-T. *J. Am. Chem. Soc.* **2002**, *124*, 6469.

[9]   (a) Tamao, K.; Uchida, M.; Izumizawa, T.; Furukawa, K.; Yamaguchi, S. *J. Am. Chem.*

Soc. **1996**, *118*, 11974.; (b) Tabatake, S.; Naka, S.; Okada, H.; Onnagawa, H.; Uchida, M.; Nakano, T.; Furukawa, K. *Jpn. J. Appl. Phys.* **2002**, *41*, 6582.; (c) Uchida, M.; Izumizawa, T.; Nakano, T.; Yamaguchi, S.; Tamao, K.; Furukawa, K. *Chem. Mater.* **2001**, *13*, 2680. (d) Palilis, L. C.; Mäkinen, A. J.; Uchida, M.; Kafafi, Z. H. *Appl. Phys. Lett.* **2003**, *82*, 2209. (e) Murata, H.; Kafafi, Z. H.; Uchida, M. *Appl. Phys. Lett.* **2002**, *80*, 189.

[10] (a) Adamovich, V. I.; Cordero, S. R.; Djurovich, P. I.; Tamayo, A.; Thompson, M. E.; D'Andrade, B. W.; Forrest, S. R. *Org. Electron.* **2003**, *4*, 77.; (b) Naka, S.; Okada, H.; Onnagawa, H.; Tsutsui, T. *Appl. Phys. Lett.* **2000**, *76*, 197.; (c)D'Andrade, B. W.; Forrest, S. R.; Chwang, A. B. *Appl. Phys. Lett.* **2003**, *83*, 3858.; (d) O'Brien, D. F.; Baldo, M. A.; Thompson, M. E.; Forrest, S. R. *Appl. Phys. Lett.* **1999**, *74*, 442.; (e) Baldo, M. A.; Lamansky, S.; Burrows, P. E.; Thompson, M. E.; Forrest, P. E. *Appl. Phys. Lett.* **1999**, *75*, 4.

[11] Ono, K.; Yanase, T.; Ohkita, M.; Saito, K.; Matsushita, Y.; Naka, S.; Okada, H.; Onnagawa, H. *Chem. Lett.* **2004**, *33*, 276.

[12] Plater, M. J.; Jackson, T. *Tetrahedron* **2003**, *59*, 4673.